Requirement for a Noncoding RNA in *Drosophila* Polar Granules for Germ Cell Establishment

Akira Nakamura, Reiko Amikura, Masanori Mukai, Satoru Kobayashi, Paul F. Lasko*

In *Drosophila* embryos, germ cell formation is induced by specialized cytoplasm at the posterior of the egg, the pole plasm. Pole plasm contains polar granules, organelles in which maternally produced molecules required for germ cell formation are assembled. An untranslatable RNA, called *Polar granule component* (*Pgc*), was identified and found to be localized in polar granules. Most pole cells in embryos produced by transgenic females expressing antisense *Pgc* RNA failed to complete migration and to populate the embryonic gonads, and females that developed from these embryos often had agametic ovaries. These results support an essential role for *Pgc* RNA in germline development.

Early cell fate specification is regulated in many animal embryos by cytoplasmic determinants that are localized asymmetrically during oogenesis. In *Drosophila*, molecules required for abdomen formation and germline establishment are localized in the posterior cytoplasm (pole plasm) of the oocyte and cleavage-stage embryo. Pole plasm contains sufficient factors required to initiate germ cell and abdomen formation (*1*). Within the pole plasm are specialized organelles called polar granules, which are composed of RNAs and proteins (*2*); similar organelles are present in germ cells throughout most of the *Drosophila* life cycle and in the germ plasm of many other animal embryos, suggesting that they have an essential role in germline formation (*3*).

Genetic screens have identified several maternally acting *Drosophila* genes with functions that are required for the formation of both abdomen and pole cells (*4*). Three of these genes, *oskar* (*osk*), *vasa* (*vas*), and *tudor* (*tud*), are central to pole plasm assembly. Mislocalization of high concentrations of *osk* RNA to the anterior pole induces functional pole plasm at the anterior (*5*). The activities of *vas* and *tud* are both required downstream of *osk* for ectopic pole cell formation, and OSK, VAS, and TUD proteins are all components of polar granules (*6*, *7*). Polar granule assembly is completed later with the localization of numerous other RNAs and proteins to the posterior cytoplasm. In contrast to *osk*, *vas*, and *tud*, which are essential both for abdomen formation and for pole cell formation, the RNAs localized later are only required for some aspects of pole plasm function. For example, *nanos* (*nos*) RNA localized in pole plasm is required for abdomen formation and for correct pole cell migration into the embryonic gonads, but not for pole cell formation per se (*8*). Two other late-localizing RNAs, mitochondrial large ribosomal RNA (mtlrRNA) and germ cell–less (*gcl*), are involved specifically in pole cell formation (*9*, *10*). However, because neither *gcl* nor mtlrRNA alone can induce pole cells at ectopic sites (*10*, *11*), it is likely that unidentified additional pole plasm components operate cooperatively with *gcl* and mtlrRNA in pole cell formation.

To identify such molecules, we used mRNA differential display to screen for RNA species that are present in wild-type embryos but absent or rare in mutant embryos that fail to form pole cells (*12*). From this screening process, we isolated a cDNA whose transcript is localized in polar granules and we named the gene *Polar granule component* (*Pgc*). *Pgc* RNA is first detectable in germarium region 2B of ovaries when it is localized in the oocyte, and it continues to be concentrated at the posterior of the oocyte until stage 7 (Fig. 1A). In stage 8, the RNA no longer accumulates in the posterior of the oocyte but instead accumulates at the anterior of the oocyte close to the oocyte–nurse cell border (Fig. 1B). Through stages 9 and 10 the RNA spreads posteriorly along the oocyte cortex (Fig. 1C), and a posterior concentration becomes detectable at stage 11 (Fig. 1D). In cleavage embryos, *Pgc* RNA is highly concentrated in pole plasm (Fig. 1E). Later, *Pgc* RNA is incorporated into pole cells, and the small amount of unlocalized *Pgc* RNA is rapidly degraded from the somatic region of the embryo (Fig. 1F). *Pgc* RNA remains detectable in pole cells until stage 10 of embryogenesis, when they pass through the posterior midgut primordium (Fig. 1G). Ultrastructural analysis revealed that *Pgc* RNA is localized in polar granules, both in

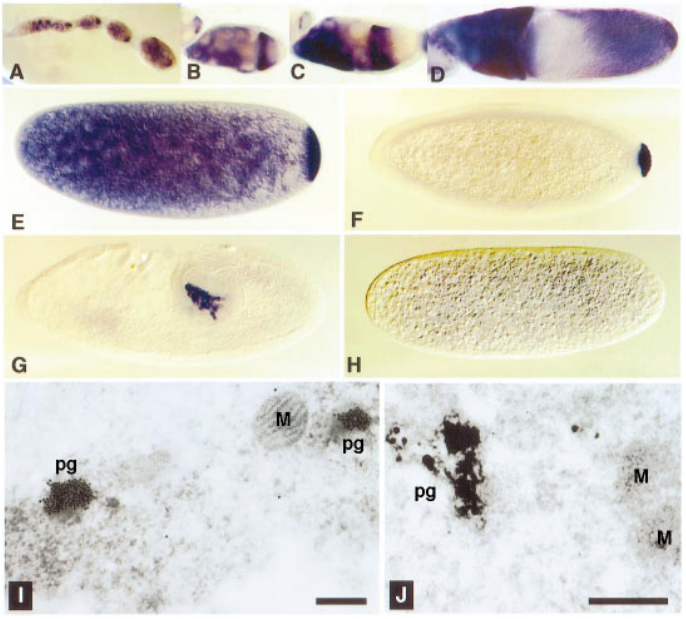

Fig. 1. Distribution of *Pgc* RNA during oogenesis and embryogenesis. (**A**) Germarium through stage 6; *Pgc* RNA is expressed from germarium region 2B and localized in the posterior region of the oocyte. (**B**) Stage 8 and (**C**) stage 9 egg chambers showing *Pgc* RNA localization to the anterior, close to the oocyte–nurse cell border. (**D**) Stage 11 egg chamber with *Pgc* RNA enriched at the posterior pole plasm of the oocyte. No detectable signal in somatic follicle cells was observed at any stage of oogenesis. (**E**) Cleavage stage embryo in which the *Pgc* RNA is highly concentrated in pole plasm. (**F**) Cellular blastoderm embryo and (**G**) stage 10 embryo with *Pgc* RNA incorporated into pole cells. (**H**) Cleavage embryo hybridized with sense *Pgc* probe as a control. (**I** and **J**) In situ hybridization examined at the electron microscopic level reveals that *Pgc* RNA is localized in polar granules in (I) the pole plasm of cleavage embryos and (J) the pole cells at the syncytial blastoderm stage. The embryo in (I) was embedded, thin-sectioned, and hybridized with a double-stranded DIG-labeled *Pgc* DNA probe after sectioning (*23*); the embryo in (J) was hybridized before embedding. In both cases the *Pgc* probe hybridized over the entire polar granule. Bar, 200 nm; M, mitochondrion; pg, polar granule.

A. Nakamura and P. F. Lasko, Department of Biology, McGill University, Montréal, Québec H3A 1B1, Canada. R. Amikura, M. Mukai, S. Kobayashi, Institute of Biological Sciences, Gene Experiment Center, and Center for Tsukuba Advanced Research Alliance (TARA), University of Tsukuba, Tsukuba, Ibaraki 305, Japan.

*To whom correspondence should be addressed. E-mail: paul_lasko@maclan.mcgill.ca

the pole plasm and in the pole cells of syncytial blastoderm embryos (Fig. 1, I and J). Within the polar granules the distribution of *Pgc* RNA differs from that of mtlrRNA. mtlrRNA is concentrated on the surface of polar granules, frequently at the boundaries between polar granules and mitochondria of early-cleavage embryos; after pole cell formation, mtlrRNA signal is undetectable on polar granules (*13*). In contrast, a *Pgc* probe hybridized throughout the entire polar granule, and signals were detected even on polar granules in pole cells.

We cloned more than 30 *Pgc* cDNAs (*14*) that hybridize to a major transcript of 0.7 kb and a minor transcript of 1.3 kb; the expression level of the larger transcript was less than 1% of that of the smaller. *Pgc* is expressed only in female germ cells. Both transcripts were detected in RNA prepared from fertile adult females, ovaries, and early-stage embryos; however, the transcripts were undetectable in RNA prepared from late-stage embryos, larvae, and pupae and from adult males and sterile females from osk^{301}/osk^{301} mothers, which produce embryos that fail to form pole cells at 25°C (*15*). Sequence analysis of the cDNAs and corresponding genomic DNA indicates that both transcripts are derived from the same

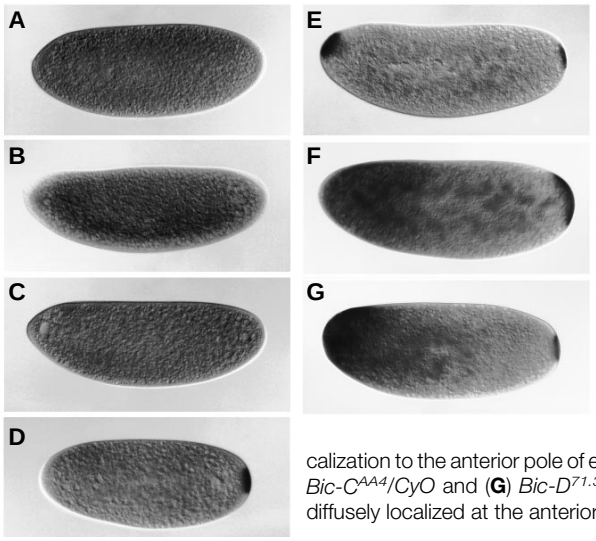

Fig. 3. Distribution of *Pgc* RNA in embryos produced by maternal patterning mutants. *Pgc* RNA is not posteriorly localized in embryos from (**A**) osk^{54}/osk^{54}, (**B**) vas^{PD}/vas^{PD}, or (**C**) tud^{WC}/tud^{WC} mothers but is normally localized in embryos from (**D**) nos^{L7}/nos^{L7} mothers. (**E**) *Pgc* RNA is mislocalized at the anterior in embryos from females carrying the *P*[ry^{+}, *osk-bcd3′UTR*] transgene (*5*). The maternal-effect *Bic-C* and *Bic-D* mutations induce a mirror-image duplication of the abdomen (but not pole cells) as a result of ectopic *osk* and *nos* localization to the anterior pole of embryos (*4, 27*). In embryos from (**F**) $Bic\text{-}C^{AA4}/CyO$ and (**G**) $Bic\text{-}D^{71.34}/Bic\text{-}D^{IIIE48}$ mothers, *Pgc* RNA is diffusely localized at the anterior.

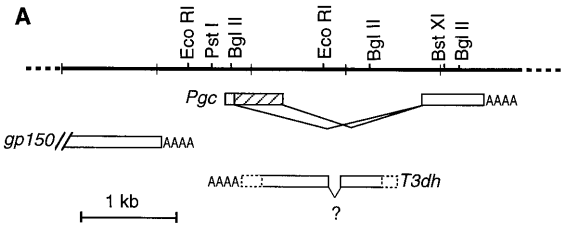

B

```
AGAATTTTGA AAGCTCAAGT ATGGTCAGAT CTTAAACGAA GATCCGTTAG TTTAACATTT  60
                          Intron
                          ▽
TTTTTTCTTC AAGAGAACAA GTTGAGCGTG GCTTTGAACT ACAAGAAGAC CCGAAAATGT 120
GCGACTACCA GATGGAGTAC TCCTTTATTT TTGAAGACAG CTCCTGCGAG GGCGATGCTC 180
GATGGCATCC TACGACAATG GATTCGAGTC CATGTGGCAT CAAGTGCGCG AGGAGTTGCA 240
AAGGGAGCGG GAGATGAATG AGCTCTGCCA GGTTTTCCAG CAAAACTTGA GCCTGAGTCC 300
GCCGGTCATC GCGGATAGAT GGAGATTCTG ACTGGACCTC CCAAAAGCCA ACTTATTGTG 360
ATATTTGTAA ATTATAGTTT TAGCAGTTCG TTTGCCACAT GAGTGGAACA TCGTGAATGC 420
ACTTTTGATA AGTGCTCGGT TATTTTATAT TGTAACTACC AGCCTTCAGA GGCGATCGTA 480
TGCATAGTTT CTTGAAGTCA ATTTGTCCGT GTATTCAAAT GTTTGCTTTC GTGAAAACTC 540
GCATTGTTTT GTCACTCTAC CAAGTAATCA ATTTGTACCA ATCAATCGCA TATGGTTGTC 600
CTAGATCTAA AAATGGCAAT AATTTGCACC TAATGTATTC AAGAACAAGG AGGGAAGCTC 660
GAAATTTCTC AAATACTTAC CCCAAAAATA GATAGAATAA TATTTTCGAT TCGCAATCGT 720
TCG(A)n                                                           723
```

Fig. 2. (**A**) Genomic organization around *Pgc*. A total of 4.8 kb of genomic sequence containing *Pgc* has been deposited in GenBank under accession number U66411. Sequence specific to the minor 1.3-kb transcript region is delineated by a striped box. The *gp150* gene (*16*) ends about 800 base pairs (bp) upstream from the *Pgc* transcription initiation site. A putative type III alcohol dehydrogenase gene [*T3dh*; BLAST scores 4.6×10^{-13} with *Bacillus methanolicus* C1 methanol dehydrogenase (*24*); 6.9×10^{-43} with a partial human cDNA clone (GenBank accession number H78978)] is transcribed from the opposite strand of sequences overlapping the *Pgc* intron and a portion of the exon specific to the 1.3-kb *Pgc* transcript (striped box). *T3dh* is transcribed in 12- to 24-hour embryos and larvae. (**B**) Nucleotide sequence of the 0.7-kb cDNA of *Pgc* (sequences corresponding to both the smaller and larger transcripts have been deposited in GenBank under accession numbers U66409 and U66410, respectively). A putative polyadenylation signal [AATATA, frequently used in *Drosophila* genes that are expressed in ovaries (*25*)] is indicated by double underlining. (**C**) Alignment of the potential translational start site for the longest ORF in the 0.7-kb *Pgc* transcript with a consensus sequence derived from actual translational start sites (*17*). Frequency refers to the percentage of actual start sites, as given in (*17*), that have the same nucleotide as does the *Pgc* sequence in the listed position. Rank refers to how frequent a particular nucleotide found in *Pgc* is in actual start sites; a value of 1 means the most common, a value of 4 means the least common. (**D**) Codon usage table for a 46–amino acid (AA) ORF (nucleotides 117 to 254) whose AUG codon is in a favorable context for translation. For all amino acids encoded by more than one codon and present in the ORF, the expected percentage (%) in *Drosophila* ORFs, as computed from published tables (*26*), is compared with the actual distribution of codons (#) in the *Pgc* ORF. Although some amino acids (notably Ser, Asp, Glu, and Cys) are encoded favorably, many others (such as Arg, Phe, Ala, Pro, Thr, and Gly) diverge substantially from *Drosophila* codon usage. The longest ORF in the minor 1.3-kb *Pgc* transcript extends for 92 codons; this ORF largely overlaps the *T3dh* coding sequence on the opposite strand and also has poor *Drosophila* codon usage.

C

G	A	U	C	G	U	A	U	G	C	*Pgc* sequence
a	c	C/A	A	a	a	A	U	G	g	Start site consensus
28	23	12	6	11	9				15	Frequency
2	3	3	3	4	4				4	Rank

D

AA	Codon	%	#	AA	Codon	%	#	AA	Codon	%	#
Phe	UUU	28	2	Pro	CCU	11	1	Asp	GAU	52	2
	UUC	72	0		CCC	37	0		GAC	48	2
					CCA	22	1				
Ile	AUU	31	1		CCG	30	0	Lys	AAA	23	1
	AUC	56	1						AAG	77	1
	AUA	13	0	Thr	ACU	14	0				
					ACC	46	0	Glu	GAA	26	1
Ser	UCU	8	0		ACA	15	1		GAG	74	2
	UCC	26	2		ACG	25	1				
	UCA	7	0					Cys	UGU	27	1
	UCG	22	1	Ala	GCU	19	1		UGC	73	4
	AGU	12	2		GCC	50	0				
	AGC	25	2		GCA	14	0	Arg	CGU	19	0
					GCG	17	1		CGC	35	0
Gln	CAA	25	0						CGA	13	1
	CAG	75	1	Tyr	UAU	32	0		CGG	14	0
					UAC	68	2		AGA	8	1
Gly	GGU	23	0						AGG	11	1
	GGC	43	2	ter	UAA	52	0				
	GGA	28	0		UAG	28	0				
	GGG	6	2		UGA	19	1				

gene (Fig. 2A). *Pgc* maps to a gene-rich area of chromosome region 58D, with the 3′ end of the *gp150* gene (*16*) less than 1 kb proximal to the 5′ end of *Pgc*. A putative type III alcohol dehydrogenase gene (*T3dh*), transcribed from the opposite strand, is nested in the *Pgc* intron and overlaps a portion of the exon specific to the minor 1.3-kb *Pgc* transcript (Fig. 2A). For the following reasons we conclude that *Pgc* encodes an untranslatable RNA. In the major 0.7-kb transcript, the longest open reading frame (ORF) (nucleotides 480 to 692; Fig. 2B) would encode a polypeptide of 71 amino acids, but its AUG codon is in an extremely poor context for translation initiation (*17*) (Fig. 2C). A shorter 46-codon ORF (nucleotides 117 to 254) begins with an AUG in a good translation initiation context, but it has poor *Drosophila* codon usage (Fig. 2D). No highly homologous [probability of a chance match, $P(N) < 10^{-4}$] sequences were obtained in BLAST searches of the nonredundant nucleic acid sequence database when any ORFs or the nucleotide sequences of either *Pgc* transcript were analyzed.

We examined embryos produced by mothers homozygous for various posterior-group mutations to determine the effects of such mutations on *Pgc* RNA localization. Embryos from *osk*, *vas*, and *tud* homozygous females failed to localize *Pgc* RNA in pole plasm (Fig. 3, A to C), and *Pgc* RNA is undetectable at the cellular blastoderm stage in these embryos. In contrast, *nos* embryos localized *Pgc* RNA normally and incorporated it into pole cells (Fig. 3D). Ectopic *Pgc* RNA localization to the anterior was observed (Fig. 3E) in embryos from females carrying the *osk-bcd3′UTR* transgene (*5*). In embryos from either *Bicaudal-C* or *Bicaudal-D* females, *Pgc* RNA was mislocalized to the anterior in a diffuse manner (Fig. 3, F and G), as has been reported for other pole plasm RNAs (*4*).

To produce flies with reduced *Pgc* function, we made transgenic lines carrying a hybrid gene in which antisense *Pgc* is expressed under the control of the *hsp70* promoter (*18*). To eliminate nonspecific deleterious effects on subsequent embryonic development, which we observed when even wild-type flies were heat shocked during mid-to-late oogenesis, in subsequent experiments we analyzed the effect of antisense *Pgc* expression on pole cell development by comparing embryos from females carrying two copies of the *hsp70-AS-Pgc* transgene (2×*AS-Pgc* embryos) cultured at constant temperature (25°C) without heat shocking. As judged by in situ hybridization with a strand-specific *Pgc* probe, the amount of localized *Pgc* RNA was greatly reduced in 2×*AS-Pgc* embryos (Fig. 4, A and B). Although *Pgc* is expressed in female germ cells throughout oogenesis, we did not observe any defect in oogenesis in females expressing antisense *Pgc*.

We analyzed the spatial distributions of several RNAs and proteins that are localized in pole plasm in 2×*AS-Pgc* embryos. The posterior concentration of all pole plasm components analyzed appeared to be essentially normal in these embryos at the cleavage stage (Fig. 4, C and D); however, in postblastodermal development, localized *nos*, *gcl*, and VAS signals were reduced in intensity (Fig. 4, E to K). Furthermore, we observed defects in pole cell migration in the 2×*AS-Pgc* embryos. In wild-type embryos, an average of 28 pole cells complete migration and associate with mesodermal tissue during stage 14 to form the two embryonic gonads (6) (Fig. 4, I, K, and M). In 2×*AS-Pgc* embryos, the ability of pole cells to complete migration and colonize the gonad is dramatically impaired (Fig. 4, J, L, and N). Three of four 2×*AS-Pgc* lines, with substantially reduced *Pgc* RNA concentrations, showed a slight reduction from 34 to between 25 and 27 in the number of VAS-positive migrating pole cells at stage 12 (Table 1). In subsequent development, many pole cells died or failed to migrate into the embryonic gonads; at stage 14 the median pole cell number was four to five

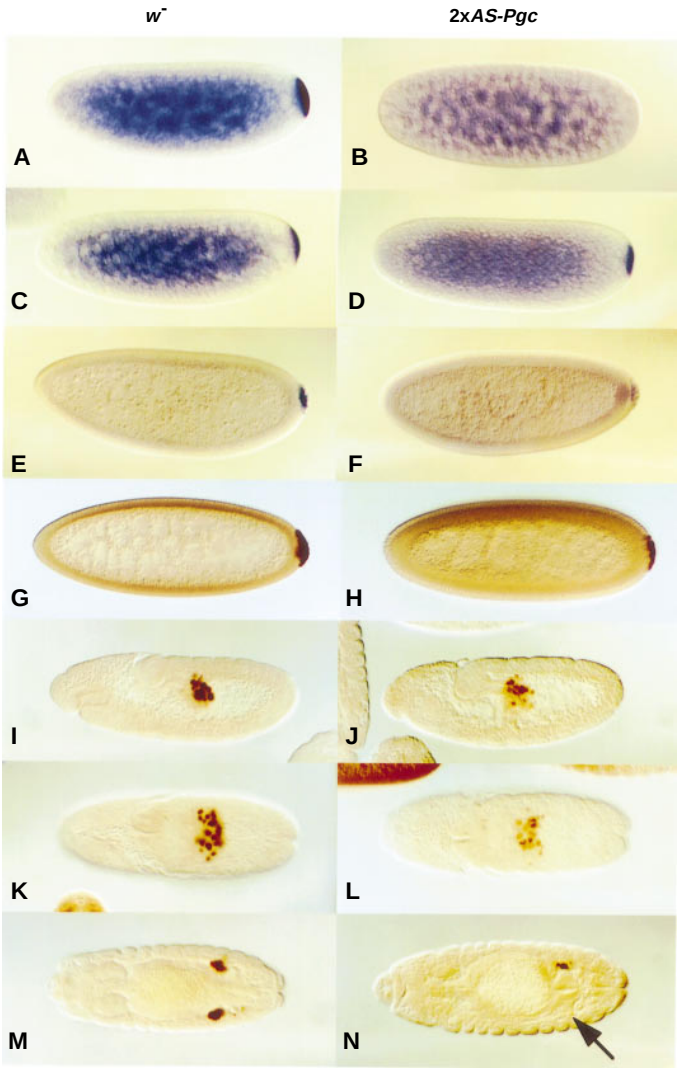

Fig. 4. Antisense *Pgc* expression affects germ cell migration and maintenance of pole plasm components. (**A**) A wild-type (w^-) embryo and (**B**) an embryo from a female carrying two copies of the *hsp70-AS-Pgc* transgene (2×*AS-Pgc* embryo) were hybridized with a *Pgc* probe. The *Pgc* signal was undetectable in 2×*AS-Pgc* embryos. (**C**) w^- and (**D**) 2×*AS-Pgc* embryos at the cleavage stage hybridized with a *gcl* probe. Initial localization of *gcl* RNA to the pole plasm is normal in 2×*AS-Pgc* embryos. (**E**) w^- and (**F**) 2×*AS-Pgc* embryos at the cellular blastoderm stage hybridized with a *gcl* probe. In 2×*AS-Pgc* embryos, signals for *gcl* in the pole cells were significantly reduced. Essentially identical results were obtained with a probe for *nos* (*28*). In (G to N), w^- and 2×*AS-Pgc* embryos are stained with affinity-purified antibody to VAS (anti-VAS). At the cellular blastoderm stage, pole cells of (**G**) w^- embryos and (**H**) 2×*AS-Pgc* embryos stain with equal intensity. At stage 10, VAS staining is noticeably weaker in (**J**) 2×*AS-Pgc* embryos than in (**I**) w^- embryos. This difference is much more obvious at stage 12 [w^- (**K**) and 2×*AS-Pgc* (**L**)]. At stage 14, pole cells are incorporated into embryonic gonads (**M** and **N**). In 2×*AS-Pgc* embryos few or no anti-VAS–stained pole cells were incorporated into the embryonic gonads (arrow points to gonads lacking pole cells). We frequently found clusters of pole cells outside of embryonic gonads in 2×*AS-Pgc* embryos (*29*). All 2×*AS-Pgc* embryos shown were embryos from females homozygous for the AS55 *AS-Pgc* insertion mated with w^- males. The AS26 and AS58 *AS-Pgc* lines gave similar results, but the AS19 *AS-Pgc* line showed no significant effects on germ cell migration or maintenance of pole plasm components. This transgene induced only a slight decrease in ovarian *Pgc* RNA concentrations and had essentially no effect on subsequent fertility (Table 1).

Table 1. Correlation between *Pgc* RNA amount and numbers of functional pole cells in progeny from females carrying two copies of the *hsp70-AS-Pgc* transgene. Relative *Pgc* RNA amount was determined by densitometric quantitation of Northern (RNA) hybridizations of a strand-specific probe to polyadenylated RNA from ovaries of the indicated lines. The filter was rehybridized with a probe for the ribosomal protein gene *RpS15a* (*30*) for loading control. Hatch rate, pole cell numbers, and ovary phenotype were scored for progeny from females of the indicated lines mated with w^- males. Agametic ovaries were frequently observed in w^- progeny from females carrying one copy of *hsp70-AS-Pgc* mated with w^- males, indicating that the agametic ovary phenotype was caused by maternally supplied antisense *Pgc* RNA.

Line	*Pgc* RNA amount (%)*	Hatching rate percent (*n*)	Number of pole cells/stage 12 embryo† (*n*)	Distribution of pole cell number in gonads of stage 14 embryos‡							Adult ovaries	
				≥6	5	4	3	2	1	0	With eggs	Agametic
w^-	100	95.8 (409)	34.2 ± 5.2 (44)	231	1	0	0	0	0	0	310	0
AS19	63	76.5 (562)	32.8 ± 5.5 (36)	175	3	2	1	1	0	0	586	12
AS26	2	94.9 (196)	27.4 ± 6.2 (55)	94	39	35	31	26	39	30	266	296
AS55	13	93.4 (455)	25.7 ± 6.5 (45)	103	35	27	30	24	18	19	275	133
AS58	40	82.9 (316)	25.0 ± 6.3 (25)	99	20	18	23	20	32	30	410	112

**Pgc* RNA amounts normalized to *RpS15a* RNA amounts and presented relative to the w^- control. †Numbers of cells that stained with affinity-purified anti-VAS. ‡Wild-type stage 14 gonads have an average of 14 pole cells (*6*).

per gonad in the three 2×*AS-Pgc* lines (Table 1). To confirm these effects on adult fertility, we examined the gonads of adult females that developed from 2×*AS-Pgc* embryos. Most embryos from these lines hatched and completed development, but, consistent with the failure of pole cells to colonize the embryonic gonads, up to 53% of adult ovaries were agametic (Table 1). These defects in germ cell proliferation correlate with a specific decrease in the amount of *Pgc* RNA (Table 1).

Our results suggest that the untranslatable *Pgc* RNA has an essential role in the differentiation of pole cells into functional, proliferative germ cells. In contrast to *gcl*, which is thought to be primarily required for pole cell formation (*9*, *11*), reduction of the *Pgc* RNA concentration has only a modest effect on initial pole cell formation. However, between stages 12 and 14, pole cells in 2×*AS-Pgc* embryos are severely compromised in their ability to migrate into the gonads and develop into functional germline stem cells. We believe that the effects we observed of antisense *Pgc* expression on germ cell establishment result from a specific interference with endogenous *Pgc* function for the following reasons: *bicoid* and *osk* RNAs were normally localized in cleavage embryos from all of the *hsp70-AS-Pgc* lines (*19*), and 2×*AS-Pgc* eggs hatched at high efficiency and developed into viable morphologically normal adults (Table 1). We hypothesize that reduction of the *Pgc* RNA concentration in the antisense lines leads to reduced stability of polar granules after their initial formation because *Pgc* RNA is an integral component of polar granules and the concentrations of various pole plasm components are reduced in postblastodermal pole cells of 2×*AS-Pgc* embryos. No abdominal defects were observed in 2×*AS-Pgc* embryos; however, because our results are based on a reduction of localized *Pgc* RNA concentrations, we cannot exclude a role for *Pgc* in abdominal specification. Null mutations may reveal additional functions for *Pgc*.

In both *Drosophila* and *Xenopus*, germ plasm can induce germ cell fate (*1*, *20*). In addition, specific components of germ plasm appear to be conserved between these two evolutionary diverse animals (*8*, *21*). A group of untranslatable RNAs, called *Xlsirts*, are localized in *Xenopus* germ plasm and are required for anchoring of *Vg1* RNA to the vegetal cortex of the oocyte (*22*). Although the exact role, if any, of *Xlsirts* in germ cell establishment is unclear, our results suggest that, like the *Xlsirts*, *Pgc* RNA functions in the maintenance of germ plasm integrity. Further analysis of the composition and role of *Drosophila* polar granules will be of relevance to understanding the molecular basis of germ cell determination in both invertebrates and vertebrates.

REFERENCES AND NOTES

1. K. Illmensee and A. P. Mahowald, *Proc. Natl. Acad. Sci. U.S.A.* **71**, 1016 (1974); H. G. Frohnhöfer, R. Lehmann, C. Nüsslein-Volhard, *J. Embryol. Exp. Morphol.* **97** (suppl.), 169 (1986); S. Sugiyama and M. Okada, *Roux's Arch. Dev. Biol.* **198**, 402 (1990).
2. A. P. Mahowald, *J. Exp. Zool*. **151**, 201 (1962).
3. _____, *ibid.* **176**, 329 (1971); E. M. Eddy, *Int. Rev. Cytol*. **43**, 229 (1975); A. P. Mahowald and S. Hennen, *Dev. Biol*. **24**, 37 (1971); M. A. Williams and L. D. Smith, *ibid.* **25**, 568 (1971); S. Strome and W. B. Wood, *Proc. Natl. Acad. Sci. U.S.A*. **79**, 1558 (1982).
4. D. St. Johnston, in *The Development of* Drosophila melanogaster, M. Bate and A. Martinez-Arias, Eds. (Cold Spring Harbor Laboratory Press, Cold Spring Harbor, NY, 1993), pp. 325–363; C. Rongo and R. Lehmann, *Trends Genet*. **12**, 102 (1996); S. Grünert and D. St. Johnston, *Curr. Opin. Genet. Dev.* **6**, 395 (1996).
5. A. Ephrussi and R. Lehmann, *Nature* **358**, 387 (1992).
6. B. Hay, L. Ackerman, S. Barbel, L. Y. Jan, Y. N. Jan, *Development* **103**, 625 (1988).
7. A. Bardsley, K. McDonald, R. E. Boswell, *ibid.* **119**, 207 (1993); W. Breitwieser, F.-H. Markussen, H. Horstmann, A. Ephrussi, *Genes Dev.* **10**, 2179 (1996).
8. C. Wang and R. Lehmann, *Cell* **66**, 637 (1991); S. Kobayashi, M. Yamada, M. Asaoka, T. Kitamura, *Nature* **380**, 708 (1996).
9. T. A. Jongens, B. Hay, L. Y. Jan, Y. N. Jan, *Cell* **70**, 569 (1992).
10. S. Kobayashi and M. Okada, *Development* **107**, 733 (1989).
11. T. A. Jongens, L. D. Ackerman, J. R. Swedlow, L. Y. Jan, Y. N. Jan, *Genes Dev*. **8**, 2123 (1994).
12. For the mutant group we used embryos from *tud*^{WC}/*tud*^{WC} females (*tud* embryos) because many of these embryos develop without extensive abdominal defects [R. E. Boswell and A. P. Mahowald, *Cell* **43**, 97 (1985)]. Total RNA was isolated from 0- to 24-hour embryos from *tud*^{WC}/*tud*^{WC} and *tud*^{WC}/*CyO* mothers as described [P. Chomczynski and N. Sacchi, *Anal. Biochem*. **162**, 156 (1987)] and used as templates for a mRNA differential display screen [P. Liang and A. B. Pardee, *Science* **257**, 967 (1992)]. After electrophoresis on 5% sequence gels, the gels were dried and processed by autoradiography. The bands of interest were cut from the gels, re-amplified with the same sets of primers as before, and cloned into pBluescript. The cDNAs were amplified by polymerase chain reaction (PCR) directly from *Escherichia coli* transformants with sets of primers corresponding to the T7 and T3 promoters (5′-CGTAATACGACTCACTATAGG-3′, and 5′-GCAATTAACCCTCACTAAAGG-3′, respectively). The spatial distributions of transcripts that were undetectable or substantially decreased in *tud* embryos were then analyzed in wild-type embryos by whole-mount in situ hybridization, essentially as described [D. Tautz and C. Pfeifle, *Chromosoma* **98**, 81 (1989)]. Digoxigenin (DIG)-labeled RNA probes were synthesized with T7 or T3 RNA polymerases in the presence of DIG-labeled uridine triphosphate (UTP) (Boehringer-Mannheim) and with PCR-amplified cDNA fragments as the templates.
13. S. Kobayashi, R. Amikura, M. Okada, *Science* **260**, 1521 (1993); R. Amikura, S. Kobayashi, H. Saito, M. Okada, *Dev. Growth Differ.* **38**, 489 (1996).
14. With the use of the partial cDNA fragment from the differential-display screen as a probe, clones were obtained from a 0- to 4-hour embryonic cDNA library [N. H. Brown and F. C. Kafatos, *J. Mol. Biol*. **203**, 425 (1988)].
15. R. Lehmann and C. Nüsslein-Volhard, *Cell* **47**, 141 (1986); A. Nakamura and P. F. Lasko, unpublished results.
16. S.-S. Tian and K. Zinn, *J. Biol. Chem*. **269**, 28478 (1994).
17. D. R. Cavener and B. A. Cavener, in *An Atlas of* Drosophila *Genes*, G. Maroni, Ed. (Oxford Univ. Press, Oxford, 1993), pp. 359–377.
18. *Pgc* cDNA corresponding to base pairs 91 to 722 of the 0.7-kb sequence shown in Fig. 2B was amplified by PCR with primers 5′-GCTTTGAACTACAAGAAGACCCG-3′ and 5′-GAACGATTGCGAATCGAAAATATATTTC-3′. The amplified fragment, which contains no *T3dh* coding sequences, was cloned into the Sma I site of pBluescript KS. A subclone in which the 5′-end of *Pgc* is adjacent to the Xba I site

was digested with Eco RI and Xba I. This fragment was subcloned into the pCaSpeR-hs vector [C. S. Thummel and V. Pirrotta, *Drosophila Inf. Serv.* **71**, 150 (1992)] to generate the *hsp70-AS-Pgc* transgene. This plasmid was introduced into the germ line of *Drosophila* with *P* element–mediated transformation [A. C. Spradling and G. M. Rubin, *Science* **218**, 341 (1982)]. Because pCaSpeR-hs contains the mini-*white* (w^+) gene, transformed w^- flies show orange to red eye color.
19. A. Nakamura and P. F. Lasko, unpublished results.
20. K. Ikenishi, S. Nakazato, T. Okuda, *Dev. Growth Differ*. **28**, 563 (1986).
21. L. Mosquera, C. Forristall, Y. Zhou, M. L. King, *Development* **117**, 377 (1993); C. Forristall, M. Pondel, L. Chen, M. L. King, *ibid.* **121**, 201 (1995); S. Kobayashi, R. Amikura, M. Okada, *Int. J. Dev. Biol*. **38**, 193 (1994).
22. M. Kloc, G. Spohr, L. D. Etkin, *Science* **262**, 1712 (1993); M. Kloc and L. D. Etkin, *ibid.* **265**, 1101 (1994).
23. For in situ hybridization, we used procedures previously described [R. Amikura, S. Kobayashi, K. Endo, M. Okada, *Dev. Growth Differ*. **35**, 617 (1993); further details of the postembedding procedure will be reported elsewhere (R. Amikura *et al.*, in preparation)].
24. G. E. deVries, N. Arfman, P. Terpstra, L. Dijkhuizen, *J. Bacteriol*. **174**, 5346 (1992).
25. V. Lantz, L. Ambrosio, P. Schedl, *Development* **115**, 75 (1992).
26. M. Ashburner (1990). *Drosophila* codon tables, version 10.0, are published electronically at http://flybase.bio.indiana.edu:82/allied-data/codons/codons.txt on the Internet.
27. R. Lehmann and C. Nüsslein-Volhard, *Development* **112**, 679 (1991); A. Ephrussi, L. K. Dickinson, R. Lehmann, *Cell* **66**, 37 (1991); M. Mahone, E. E. Saffman, P. F. Lasko, *EMBO J*. **14**, 2043 (1995).
28. A. Nakamura and P. F. Lasko, unpublished results.
29. A. Nakamura, R. Amikura, M. Mukai, S. Kobayashi, P. F. Lasko, data not shown.
30. C. Lavoie *et al.*, *J. Biol. Chem*. **269**, 14625 (1996).
31. We thank A. Ephrussi for providing us the *osk* cDNA clone and for the *osk-bcd3′UTR* lines, H. Foley for secretarial assistance, and C. Lévesque for fly food preparation. Supported by research grants from Natural Sciences and Engineering Research Council of Canada and the National Cancer Institute of Canada (NCIC), with funds from the Canadian Cancer Society. A.N. is a Japan Society for the Promotion of Science postdoctoral fellow. P.L. is a Research Scientist of the NCIC.

21 August 1996; accepted 23 October 1996

Evidence for the Conformation of the Pathologic Isoform of the Prion Protein Enciphering and Propagating Prion Diversity

Glenn C. Telling, Piero Parchi, Stephen J. DeArmond, Pietro Cortelli, Pasquale Montagna, Ruth Gabizon, James Mastrianni, Elio Lugaresi, Pierluigi Gambetti, Stanley B. Prusiner*

The fundamental event in prion diseases seems to be a conformational change in cellular prion protein (PrP^C) whereby it is converted into the pathologic isoform PrP^{Sc}. In fatal familial insomnia (FFI), the protease-resistant fragment of PrP^{Sc} after deglycosylation has a size of 19 kilodaltons, whereas that from other inherited and sporadic prion diseases is 21 kilodaltons. Extracts from the brains of FFI patients transmitted disease to transgenic mice expressing a chimeric human-mouse PrP gene about 200 days after inoculation and induced formation of the 19-kilodalton PrP^{Sc} fragment, whereas extracts from the brains of familial and sporadic Creutzfeldt-Jakob disease patients produced the 21-kilodalton PrP^{Sc} fragment in these mice. The results presented indicate that the conformation of PrP^{Sc} functions as a template in directing the formation of nascent PrP^{Sc} and suggest a mechanism to explain strains of prions where diversity is encrypted in the conformation of PrP^{Sc}.

For many years the prion diseases, also called transmissible spongiform encephalopathies, were thought to be caused by slow-acting viruses (*1*), but it is now clear that prions are not viruses and that they are devoid of nucleic acid (*2, 3*). Prions seem to be composed only of PrP^{Sc} molecules, which are abnormal conformers of a normal, host-encoded protein designated PrP^C (*3, 4*). PrP^C has a high α-helical content and is virtually devoid of β-sheets, whereas PrP^{Sc} has a high β-sheet content (*4, 5*); thus, the conversion of PrP^C into PrP^{Sc} involves a profound conformational change. Formation of PrP^{Sc} is a posttranslational process that does not appear to involve a covalent modification of the protein (*6*).

The prion diseases are unique in that they may present as inherited and infectious disorders (*3, 7*). More than 20 different mutations of the human (Hu) PrP gene segregate with dominantly inherited disease; five of these have been genetically linked to familial Creutzfeldt-Jakob disease (fCJD), Gerstmann-Sträussler-Scheinker disease, and fatal familial insomnia (FFI) (*8*). The most common prion diseases of animals are scrapie of sheep and bovine spongiform encephalopathy; the latter may have been transmitted to people through foods (*9*).

To extend studies on the transmission of wild-type and mutant prions from sporadic Creutzfeldt-Jakob disease (sCJD) and fCJD patients, respectively, to transgenic mice expressing a chimeric mouse-human PrP gene [Tg(MHu2M) mice] (*10, 11*), we inoculated these mice with mutant prions from the brains of patients who died of FFI. Transmission of human prions to Tg(MHu2M) mice involves the conversion of chimeric MHu2M PrP^C into MHu2M PrP^{Sc} through a process that is thought to involve the binding of PrP^{Sc} to PrP^C as PrP^C undergoes a structural transition (*12, 13*). A point mutation of the PrP gene at codon 178 [in which an Asp residue at position 178 is mutated to Asn (D178N)] is the cause of FFI, but a Met residue must be encoded at position 129 on the mutant allele for the FFI phenotype to be manifest (*14*). The same D178N mutation segregates with a subtype of fCJD, but in this case, Val is encoded on the mutant allele at position 129. The D178N mutation is thought to destabilize the structure of PrP^C, resulting in its transformation into PrP^{Sc} (*13, 15*). Some investigators have reported transmission of FFI prions to non-Tg and Tg(HuPrP) mice; the incubation times exceeded 400 days, and only a minority of the inoculated Tg(HuPrP) mice expressing both human and mouse PrP^C developed disease (*16*). These findings with Tg(HuPrP) mice are in accord with earlier studies showing that transmission of human prions to Tg(HuPrP) mice is inhibited by mouse PrP^C, and this inhibition can be abolished by ablation of the mouse PrP gene ($Prnp^{0/0}$) (*10, 11*).

Tg(MHu2M)$Prnp^{0/0}$ mice (*17*) were inoculated intracerebrally with extracts prepared from brain tissue obtained after the death of individuals who died of FFI, fCJD(E200K) (with a mutation in which Glu at position 200 has mutated to Lys), or sCJD. The mice developed signs of experimental prion disease about 200 days after inoculation (Table 1). At the time of writing, inoculation of Tg(MHu2M)$Prnp^{0/0}$ mice has resulted in primary passage of prions from at least one brain region from

G. C. Telling and J. Mastrianni, Department of Neurology, University of California, San Francisco, CA 94143, USA.
P. Parchi and P. Gambetti, Division of Neuropathology, Department of Pathology, Case Western Reserve University, Cleveland, OH 44106, USA.
S. J. DeArmond, Departments of Neurology and Pathology, University of California, San Francisco, CA 94143, USA.
P. Cortelli, P. Montagna, E. Lugaresi, Department of Neurology, University of Bologna, Bologna 40123, Italy.
R. Gabizon, Department of Neurology, Hadassah Medical Center, Hebrew University, Jerusalem 91120, Israel.
S. B. Prusiner, Departments of Neurology and Biochemistry and Biophysics, University of California, San Francisco, CA 94143, USA.

*To whom correspondence should be addressed at the Department of Neurology, HSE-781, University of California, San Francisco, CA 94143–0518, USA.

Requirement for a Noncoding RNA in *Drosophila* Polar Granules for Germ Cell Establishment

Akira Nakamura, Reiko Amikura, Masanori Mukai, Satoru Kobayashi and Paul F. Lasko

Science **274** (5295), 2075-2079.
DOI: 10.1126/science.274.5295.2075